Hydrogen-Bonded Double Strands: Crystal Structure and Spectroscopic Properties of a 2,2′-Dipyrryl Ketone

Michael T. Huggins, Adrianne K. Tipton, Qingqi Chen,
and **David A. Lightner**[*]

Department of Chemistry, University of Nevada, Reno, NV 89557-0020, USA

Summary. The synthesis, crystal structure determination, conformational analysis, and spectroscopic properties of 3,3′-diethyl-4,4′-dimethyl-2,2′-dipyrryl ketone (**1**) are reported. The dipyrryl ketone is a model for the dipyrrole core of 10-oxobilirubin, a presumed metabolite in alternate pathways of excretion of the yellow pigment of jaundice, bilirubin. In the crystal, **1** adopts a helical conformation, with a molecule of one helicity being hydrogen-bonded to two molecules of the opposite helicity. Thus, **1** self-assembles *via* hydrogen bonding into supramolecular double-stranded arrays, where molecules of the same helicity comprise one strand and are paired through hydrogen bonding to molecules of opposite helicity in the second strand. In the observed molecular conformation each pyrrole ring and adjacent carbonyl group are rotated into an *sc* conformation (torsion angle $\sim 29°$), with each N-H pointing in the same direction as the C=O. Molecular mechanics/dynamics calculations predict the *sc,sc* conformation, absent hydrogen bonding, to be the most stable, but only by a few tenths of a kj/mol. In $CHCl_3$, **1** is monomeric according to vapor pressure osmometry studies ($MW_{obs} = 251 \pm 10$ *vs.* $MW_{calc} = 244$). ^{1}H NMR NH chemical shifts in $CDCl_3$ suggest a predominantly *anti* orientation of the C=O and pyrrole NHs, which is opposite to the orientation observed in the crystal.

Keywords. Pyrrole; Conformation; Hydrogen bonding.

Introduction

Bilirubin (Fig. 1) is the yellow pigment of jaundice [1, 2]. In healthy adults some 300 mg of bilirubin are produced each day and secreted by the liver into bile as glucuronide conjugates [1]. 10-Oxo-bilirubin (Fig. 1) has been suggested as a metabolite formed in alternative (oxidative) pathways for elimination of bilirubin [3]. Whereas the structure, metabolism, and photochemistry of bilirubin have received much attention in recent years, far less is known of 10-oxobilirubin. Much of what we know of the properties of bilirubin was anticipated through stereochemical and photochemical studies of its dipyrrole analogs, dipyrrinones and dipyrrylmethanes (Fig. 1), and most of the stereochemical studies of these dipyrrolic analogs come from X-ray crystallography and molecular mechanics calculations [4]. The first and
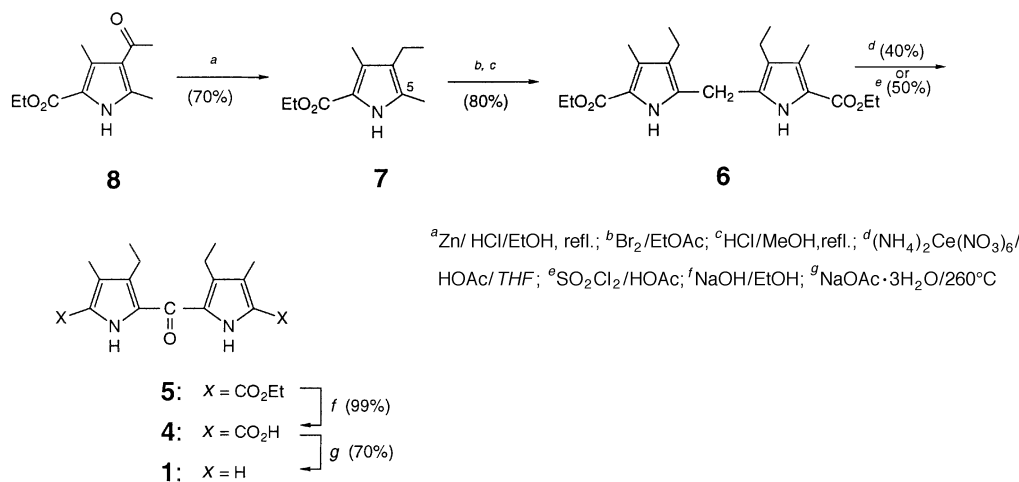
---

[*] Corresponding author
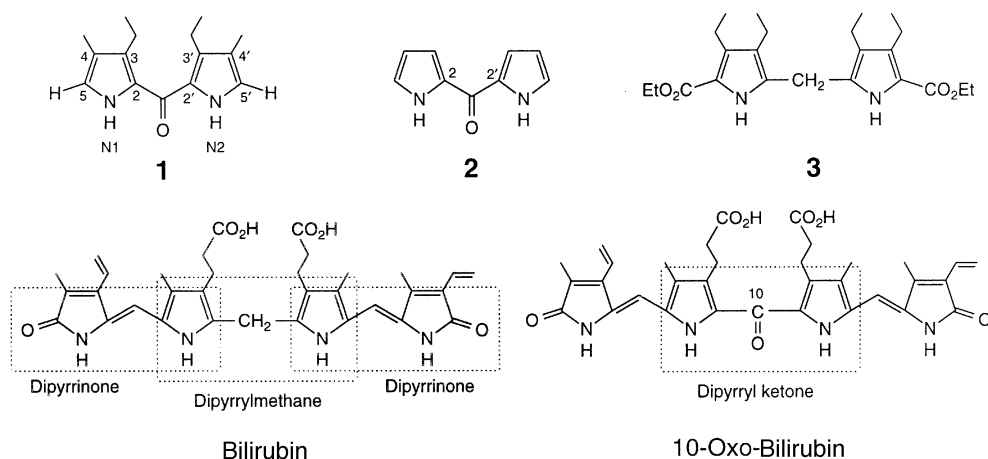
Fig. 1. Constitutional structures of dipyrrylketone analogs (**1** and **2**) of 10-oxobilirubin and a dipyrrylmethane (**3**) analog of bilirubin

only crystal structure of a dipyrrylmethane (**3**) was presented by *Bonnett et al.* [5]. This was followed by crystal structures of bilirubin [6] and several dipyrrinones [7]. Conformational analysis of dipyrrylmethanes and dipyrrinones was provided by CNDO/2 molecular orbital calculations and by molecular mechanics methods [4, 8]. Until very recently, however, there was little information available on the stereochemistry of dipyrryl ketone analogs of 10-oxobilirubin. A crystallographic structure of the parent compound, 2,2′-dipyrryl ketone (**2**), indicated a preference for the *sp,sp* conformation, with one pyrrole NH and the carbonyl participating in intermolecular hydrogen bonding [9]. Interestingly, molecules of **2** in the crystal are arranged in supramolecular helicies, and, like benzil [10], all molecules have the same helicity in a given crystal. However, the relevance of this information to the stereochemistry of 10-oxobilirubin is unclear, given that the latter has pyrrole β-substituents that might tend to sterically disfavour the *sp,sp* conformation observed for **2**. In the following we report on the synthesis, crystal structure, and conformational analysis of the β-substituted dipyrryl ketone **1**.

Results and Discussion

Synthetic aspects

Our approach to the preparation of **1**, as outlined in Scheme **1**, involved conversion of a suitable monopyrrole (**7**) to a dipyrrylmethane (**6**) [11], followed by oxidation to an oxo-dipyrrylmethane (**5**) and then removal of the carboethoxy groups. Thus, the target dipyrryl ketone **1** was synthesized in six steps from the readily available monopyrrole **8** [12], which was conveniently reduced to **7** under *Clemmensen* conditions [13]. Monobromination of the C(5) methyl group of **7** was accomplished using bromine in ethyl acetate, and the resulting bromomethyl derivative was solvolyzed in methanolic hydrochloric acid to afford **6** [11, 14] in high yield. Oxidation of the central methylene group of **6** could be achieved in comparable yield either by treatment with ceric ammonium nitrate [15] or by reaction with

^{a}Zn/ HCl/EtOH, refl.; ^{b}Br$_2$/EtOAc; ^{c}HCl/MeOH,refl.; ^{d}(NH$_4$)$_2$Ce(NO$_3$)$_6$/ HOAc/ *THF*; ^{e}SO$_2$Cl$_2$/HOAc; ^{f}NaOH/EtOH; ^{g}NaOAc·3H$_2$O/260°C

Scheme 1

sulfuryl chloride followed by hydrolysis [16]. Although **5** could be saponified easily and in high yield to **4**, the dicarboxylic acid resisted decarboxylation by conventional methods. However, we found that **4** underwent smooth loss of CO$_2$ in molten sodium acetate trihydrate to give **1**.

Molecular geometry from X-ray crystallography and molecular dynamics calculations

Previously, only two related dipyrrole structures had been established by X-ray analysis: dipyrrylmethane **3** [5] of Fig. 1 and the simplest 2,2′-dipyrryl ketone (**2**) [9]. Both exhibit intermolecular hydrogen bonding in the crystal: monoclinic **3** as hydrogen-bonded dimers, orthorhombic **2** as a hydrogen-bonded oligomer. The latter is particularly interesting, as individual crystals are homochiral, with molecules of **2** all having the same helicity (torsion angles $\phi_1 \sim 13°, \phi_2 \sim 10°$) and being arrayed along a helical chain (Fig. 2A) with intermolecular hydrogen bonding linking one molecule to the next.

The crystal structure of **1** is rather different from that of **2**. Two crystallographically unique molecules (**A** and **B**, Fig. 2B) of **1** are found in the unit cell Fig. 3A). **A** and **B** have nearly mirror image shapes but are not true enantiomers; and they are organized very differently in the crystal, as compared with **2**. Molecules of **1** do not fall into helical arrays with each molecule hydrogen bonded to the next but are arranged in strands consisting of only **A** or only **B** conformers. Side-by-side **A** molecules in one strand are tethered by a network of hydrogen bonds to side-by-side **B** molecules in a second strand (Fig. 2B), and these double strands extend indefinitely through the crystal lattice. Although the **A** molecules are not hydrogen bonded to other **A** molecules, nor are **B** hydrogen bonded to **B**, each molecule of one strand is hydrogen bonded to *two* molecules of the second strand of the duplex using both NHs and the carbonyl of each molecule. Thus, in the crystal structure of **1** there are four hydrogen bonds to each molecule, whereas in **2** there are only two, as only one NH is used in hydrogen bonding. As with **2**, the

(A)

(B)
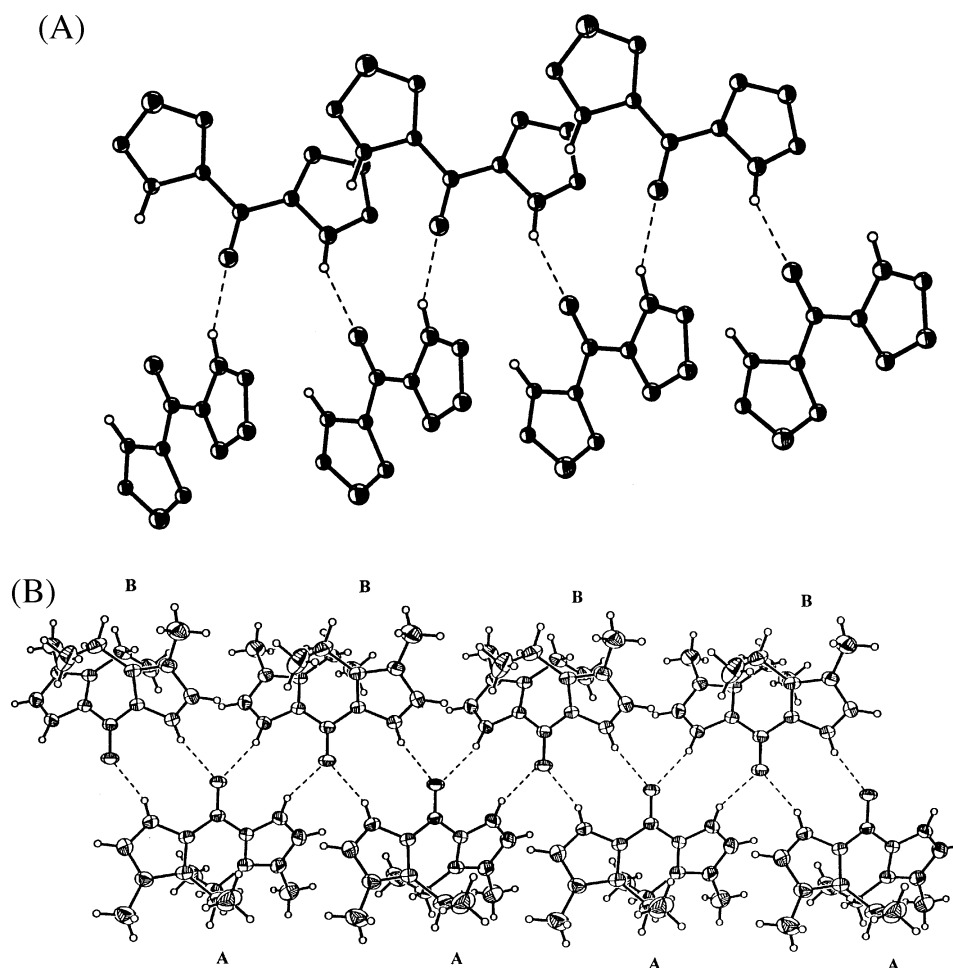
Fig. 2. (A) Ball and stick (Ref. 4) representation of 2,2′-dipyrryl ketone (**2**) in an intermolecularly hydrogen-bonded helical array in its crystal [9]. All molecules of **1** adopt the *sp,sp* conformation and all have the same helicity. (B) Crystal structure drawing of **1** showing strands of **A** and **B** molecules, with each **A** molecule hydrogen-bonded to two **B** molecules, and each **B** molecule hydrogen-bonded to two **A** molecules. **A** and **B** have opposite helicity and similar *sc,sc* conformations but are not enantiomers
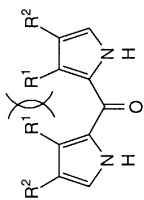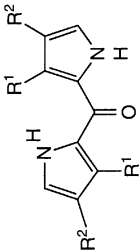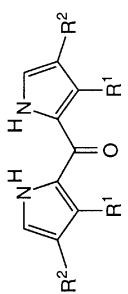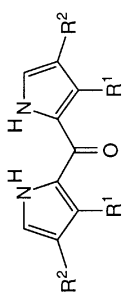
N to O nonbonded distances of the N–H···O=C hydrogen bond are 2.89 to 2.92 Å, which equals approximately the sum (2.90 Å) of the *van der Waals* radii of O and N. Molecules **A** and **B** are more twisted (helical) than those of **2**, with torsion angles {$\phi_1 \sim \phi_2 \sim 29°$ in **A** and $\phi_1 \sim -25°$, $\phi_2 \sim -32°$ in **B** (*vs.* $\phi_1 \sim 13°$, $\phi_2 \sim 10°$ in **2**). Thus, crystals of **1** are not homochiral as in **2**, and intramolecular steric repulsion between pyrrole β-alkyl groups of adjacent rings (3,3′ of Fig. 1) apparently increases the torsion angles and hence the interplanar angle of **1** (**A**: 59°, **B**: 62°), which is about twice as large as that of **2** (25°).

Molecular dynamics calculations indicate a slight preference for the *ac,sc* conformation of **1** (Table 1) over the *sc,sc* and *ac,ac* conformers. The computed differences are too small to be meaningful. The *sc,sc* conformation with $\phi_1 \sim 37°$, $\phi_2 \sim 36°$ is only 0.8 kj/mol higher in energy than the *ac,-sc*, and this *sc,sc*

(A)

(B)
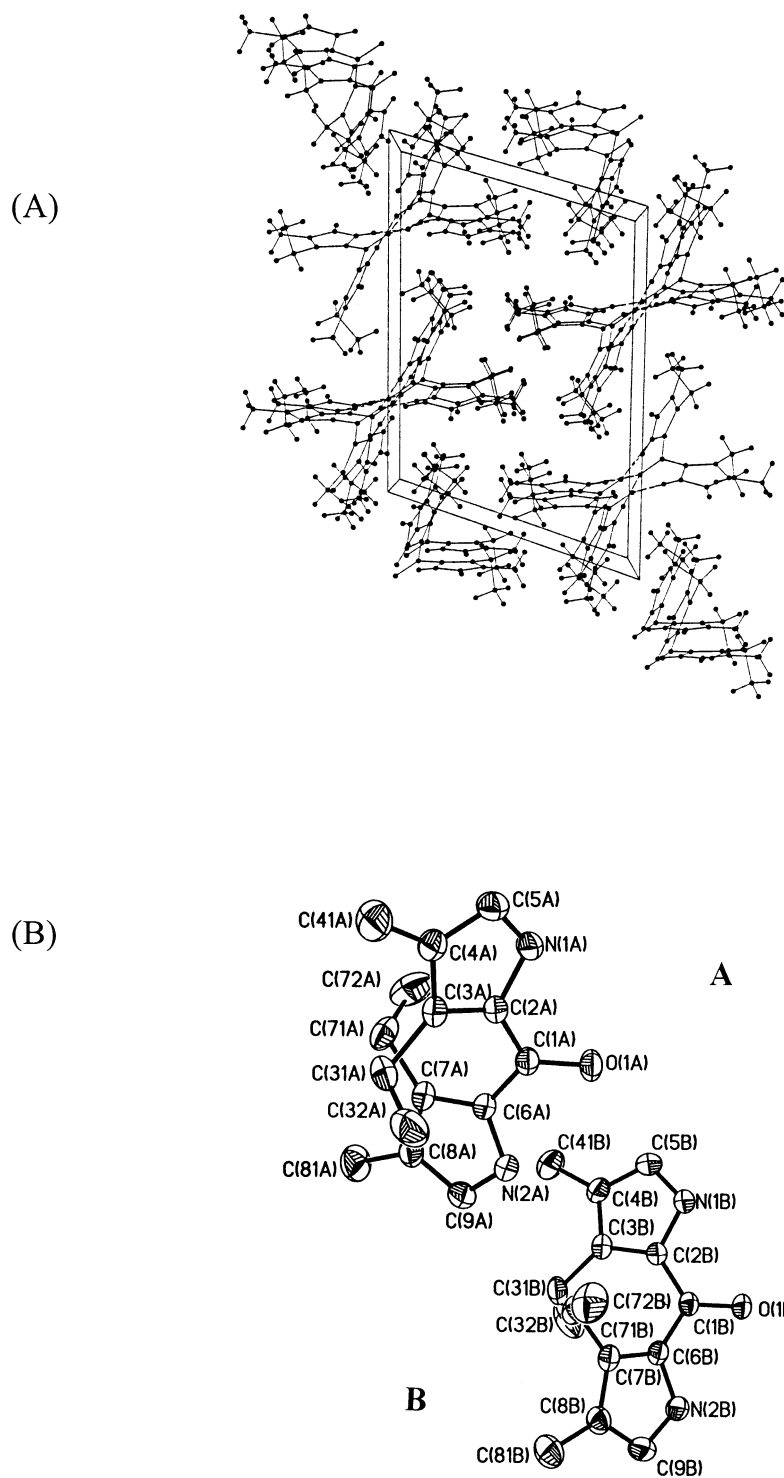
Fig. 3. (A) Molecular packing and unit cell of **1** in the projection (010), viewed down the *b* axis. (B) The numbering system used in the crystal structure of **1** shown for carbon, nitrogen, and oxygen (O) atoms of **A** and **B**

Table 1. Conformation-determining torsion angles in **1** and **2**[a] from molecular dynamics calculations[b]

Compound	Stereochemistry	Method	Torsion angles (°) ϕ_1 (N(10)-C-C=O)	ϕ_2 (O=C-C-H(11))	Interplanar angle (°)	Energy difference[c] (kJ/mol)
	1 *sc,sc*	X-ray	29	29	59,62	–
	2 *sp,sp*	X-ray	13	10	25	–
	1 *sc,sc*	MD	37	36	63	0.8
	2 *sp,sp*	MD	8	8	14	0.0
	1 *ac,-sc*	MD	149	−30	41	0.0
	2 *ac,-sp*	MD	162	−13	28	5.9
	1 *ac,ac*	MD	156	157	53	1.7
	2 *ac,ac*	MD	157	157	40	13.4

[a]**1**: R^1 = Et, R^2 = Me; **2**: $R^1 = R^2$ = H; [b]molecular dynamics (MD) calculations using Sybyl vers. 6.4 on an SGI Octane workstation; [c]compare the three conformers of **1** or the three conformers of **2**, no cross-correlation of total steric energy differences between **1** and **2**
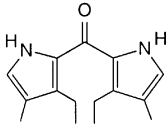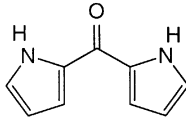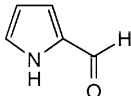
conformation is very close to that seen in the crystal. There is no strong energy bias against the *ac,ac* conformer, which is the conformation adopted by the central dipyrrole core of bilirubin, and probably by its 10-oxo analog (Fig. 1). In contrast, molecular dynamics calculations of **2** indicate a strong bias for the *sp,sp* conformer, nearly the same as that found in the crystal, over the *ac,-sp* and the *ac,ac* conformers. Although only one of the two pyrroles of **2** is involved in hydrogen bonding in the crystal, the computations provide a rationale for finding only the *sp,sp* conformer in the crystal lattice.

Substituents at the pyrrole β-positions, especially at 3 and 3′, might be expected to destablize the *sp,sp* conformation by steric repulsions between the R' groups (Table 1). Molecular dynamics calculations on **1** support an *sc,sc* conformation over *sp,sp*, but the *sc,sc* conformation is destabilized by steric repulsions and thus closer in energy to the *ac,-sc* and *ac,ac* conformations that are disfavoured in **2**.

State of aggregation in solution

Vapor pressure osmometry (VPO) measurements have proven useful in detecting aggregation of pyrrolic compounds in solution, especially linear di- and tetrapyrroles [4, 17]. In dimerization-promoting non-polar solvents such as chloroform, dipyrrinones form tight dimers, and bilirubin diesters are mainly dimeric, probably through the action of intermolecular hydrogen bonding. In our studies, in which we used benzil as a calibration standard, we found that **1** is monomeric in chloroform solution in the range of $2.8 - 8.2 \times 10^{-3}$ mol/kg (Table 2). VPO measurements also indicate that **2** and its monopyrrole analog, pyrrole α-aldehyde, are monomeric in chloroform.

Table 2. Molecular weights[a] of related pyrroles (**1**, **2**, and pyrrole α-aldehyde in CHCl$_3$ at 45°C)

	Actual MW	Observed MW	Conc. Range (mol/kg)
1	244	251±10	$2.8-8.2\times10^{-3}$
2	160	164±10	$4.1-13.2\times10^{-3}$
Pyrrole α-aldehyde	95	89±10	$1.1-3.2\times10^{-2}$

[a] Benzil (MW 210) served as the calibration standard, giving an observed molecular weight of 220±15 for a concentration range of $3.9-17.7\times10^{-3}$ mol/kg

Hydrogen bonding in solution

From ^{1}H NMR spectroscopy, pyrrole NH signals can often reveal information on hydrogen bonding, both intramolecular and intermolecular [4, 17, 18]. Since VPO studies of **1** and **2** indicate monomeric solutions, it remained to be seen whether intramolecular hydrogen bonding could be detected. Consistent with monomeric solutions, the N–H chemical shifts (Table 3) of **1**, **2**, and pyrrole α-aldehyde show little variation over a 100-fold difference in concentration, and the chemical shifts are nearly the same for each of these compounds at the same concentration. Since we have no model compounds similar to those of Table 3 that are (or are not) conclusively intramolecularly hydrogen-bonded, we turned to an examination of the N–H stretch in their infrared spectra. *Kuhn* and *Kleinspehn* [19] have observed that for a series of dipyrrylmethane diesters, **9** exhibited N–H stretching in carbon tetrachloride near $3450\,cm^{-1}$, whereas **10** exhibited two bands, one near $3450\,cm^{-1}$ and the other near $3350\,cm^{-1}$, and **11** exhibit only one band near $3400\,cm^{-1}$ (Table 4). Compound **9** is incapable of intramolecular hydrogen bonding, and its v_{N-H} is at $3458\,cm^{-1}$, but **10** can adopt a conformation where the N–H ($v_{N-H} = 3361\,cm^{-1}$) of one pyrrole ring hydrogen bonds to the α-carboethoxy carbonyl on the other pyrrole ring, leaving one N–H ($v_{N-H} = 3466\,cm^{-1}$) free of hydrogen bonding. The hydrogen-bonded N–H appears at lower wavenumber as expected. In **11**, both pyrrole N–Hs can engage in hydrogen bonding, each to a carboethoxy group of the opposing ring, hence $v_{N-H} = 3397\,cm^{-1}$. The N–H stretching data for **1**, **2**, and pyrrole α-aldehyde all show the higher wavenumber band near $3450\,cm^{-1}$, and none of them shows a band corresponding to hydrogen-bonded N–H. Consequently, we believe that both **1** and **2** are monomeric in solution and neither engages in intramolecular hydrogen bonding.

Conformation in solution

It is difficult to assess the conformation of dipyrryl ketones in solution. So far as we are aware, there is relatively little information as to whether the ketone carbonyl prefers to be *anti* to the pyrrole NHs, or *syn* as required for intermolecular hydrogen bonding and observed in crystals of **1** and **2**. A study of NH chemical shifts in the ^{1}H NMR spectra of 2-pyrryl ketones and esters (Table 5) suggests a way to distinguish *syn* and *anti* conformations. In the *syn* orientation, the N–H lies in a carbonyl deshielding cone [20] and is thus expected to appear $\sim 1\,ppm$
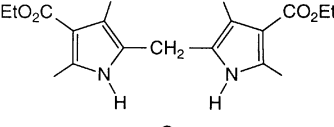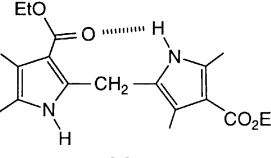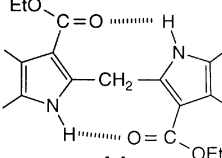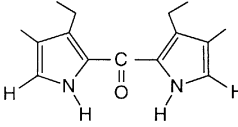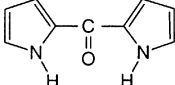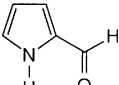
Table 3. Concentration dependence of the NH ^{1}H NMR chemical shifts (ppm) of **1**, **2**, and pyrrole α-aldehyde in CDCl$_3$ at 25°C

Concentration (*M*)	Pyrrole NH Chemical Shift (δ, ppm)[a]		
	Dipyrryl Ketone **1**	Dipyrryl Ketone **2**	Pyrrole α-Aldehyde
0.01	8.51	9.50	9.64
0.001	8.49	9.43	9.58
0.0001	8.49	9.40	9.55

[a] Downfield from *TMS* at 500 MHz

Table 4. Comparison of infrared N-H stretching vibrations (cm^{-1}) in selected dipyrrylmethanes and dipyrryl ketones[a]

9	10	11
3458	3466, 3361	3397

1		
3454	3451	3453

[a] In CCl_4 at ∼10^{-2} M; [b] data from Ref. 19

Table 5. Observed NH chemical shifts (δ_{NH}, ppm)[a] for pyrrole α-aldehydes, ketones, and esters in CDCl$_3$ $vs.$ heats of formation for syn and $anti$ conformers

| | syn | | | $anti$ | syn | | | $anti$ | |
| | | | | | | | | | |
R	δ_{N-H}	$\Delta\Delta H_f^b$ (kj/mol)	ϕ_{syn}^c (°)	ϕ_{anti}^c (°)	δ_{N-H}	$\Delta\Delta H_f^b$ (kj/mol)	ϕ_{syn}^c (°)	ϕanti^c (°)
H[d]	9.6	11.3	0	180	9.4[f]	11.7	0	149
Me[d]	9.4	7.9	0	180	8.9[f]	−0.8	39	137
OMe[d]	9.2	−1.5	0	180	8.8[g]	4.2	26	156
tBu[e]	9.6	−3.6	0	125	8.6[h]	–	–	115

[a] Downfield from TMS; [b] difference in heat of formation ($\Delta H_f(syn) - \Delta H_f(anti)$) as determined by PCModel molecular mechanics calculations using the MMX forcefield (Serena Software, Bloomington, Indiana, USA); [c] Torsion angles N–C–C=O for syn or $anti$ isomers in their minimum energy conformations determined from PCModel molecular mechanics calculations; [d] Fischer H, Orth H (1934) Die Chemie des Pyrrols, Akademische Verlagsgesellschaft mbH, Leipzig, vol I, pages 152 (R=H), 183 ($R = CH_3$), and 237 ($R = OCH_3$); [e] Mirachi D, Ritchie GLD (1984) J Mol Struct **116**: 337; [f] Fischer H, Hofelmann H (1938) Liebigs Ann Chem **533**: 216; [g] Manitto P, Monti P (1980) J Chem Soc Chem Commun 178 (for the ethyl ester); [h] New compound, prepared by reaction of 3,4-dimethylpyrrole $Grignard$ with pivaloyl chloride to give the pyrryl ketone of the correct molecular weight and spectroscopic data

downfield of the N–H when the orientation is *anti*. An especially nice example may be found in the *cisoid* α, β-unsaturated ($H_2C=C-C=O$) ketone of the natural product lemnalol, where the olefinic *syn* hydrogen, which lies in the same position relative to the carbonyl group as in *sp*- or *sc*-**1**, resonates at 6.01 ppm, whereas the *anti* proton appears at 5.04 ppm [21].

Experimental

All UV/Vis spectra were recorded on a Perkin-Elmer λ-12 spectrophotometer, infrared spectra were measured on a Perkin-Elmer Spectrum BX FT-IR system, and all nuclear magnetic resonance (NMR) spectra were obtained on a GE QE-300 300-MHz spectrometer. Chemical shifts are reported in δ (ppm) referenced to the residual CHCl$_3$ [1]H signal at 7.26 ppm and the ^{13}C signal at 77.0 ppm. Melting points were taken on a Mel-temp capillary apparatus and are uncorrected. Vapor pressure osmometry measurements were performed on a Gonotec Osmomat 070 osmometer calibrated with benzil at 45°C in CHCl$_3$. Combustion analysis of **1** was performed by Desert Analytics, Tucson, AZ, giving data in satisfactory agreement with the calculated values. Analytical thin layer chromatography was carried out on J. T. Baker silica gel IB-F plates (125 μ layers). Spectroscopic data were obtained in spectral grade solvents (Aldrich or Fisher). Bromine and ceric ammonium nitrate (*CAN*) were purchased from J. T. Baker Co., trifluoroacetic acid, ethyl acetate, and sulfuryl chloride from Acros Organics, dichloromethane, methanol, and acetic acid from Fisher. The crystalline starting material, ethyl 4-acetyl-3,5-dimethylpyrrole 2-carboxylate (**8**), is readily available (74% yield) by a *Fischer-Knorr* type reaction of the oxime of ethyl acetoacetate with pentan-2,4-dione in the presence of zinc powder [12]. The acetyl group of **8** can be smoothly reduced using zinc in methanolic hydrochloric acid to afford 60% or higher [13] yields of ethyl 3,5-dimethyl-4-ethylpyrrole 2-carboxylate (**7**). The latter served as the immediate precursor to dipyrrylmethane **6**, whose improved synthesis in 80% yield is reported below. Previously [15a], we had reported on the conversion of **6** to dipyrryl ketone **5** in ∼60% yield using ceric ammonium nitrate (*CAN*) as oxidizing agent [15b]. In the current study, **5** was saponified in 99% yield and decarboxylated in 70% yield to afford the target dipyrryl ketone **1** [16]. In the following, we report improved methods or yields for **6** and **1** from their immediate precursors.

3,3′-Diethyl-4,4′-dimethyl-5,5′-bis-(ethoxycarbonyl)-2,2′-dipyrrylmethane (**6**; C$_{21}$H$_{30}$N$_2$O)

Ethyl 3,5-dimethyl-4-ethylpyrrole 2-carboxylate (**7**, 14.4 g, 73.8 mmol), prepared from **8** as described previously [13], was dissolved in 100 cm^3 ethyl acetate; then 11.8 g Br$_2$ (73.8 mmol, 1.0 equiv.) were added dropwise over 15 min. After all the Br$_2$ had been added, a considerable amount of a yellow solid had precipitated from the solution. The mixture was allowed to stir for another hour at room temperature before removing the solvent to dryness using a rotary evaporator. The yellow solid residue was dissolved directly in 100 cm^3 methanol containing 2 cm^3 of conc. hydrochloric acid. The amount of solvent used is a key factor in leading to a good yield. Too much solvent leads to low yields of product; the less solvent, the better the result. The mixture was heated to reflux for 1 h before cooling to 0°C and adjusting the *pH* to 7 using 10% aqueous ammonia. The resulting white precipitate was collected by suction filtration and recrystallized from 70% aqueous methanol to yield the desired compound.

Yield: 11 g (80%); m.p.: 125–126°C (Lit.: m.p.: 122–123°[14], 124–125°C [22], 126–127°C [23], 126°C [24]; IR (film): $\nu =$ 3313, 2963, 2928, 2869, 1652, 1444, 1278, 1252 cm^{-1}; ^{1}H NMR (CDCl$_3$, δ, 300 MHz): 1.04 (t, $J =$ 6.0 Hz, 6H), 1.29 (t, $J =$ 7.3 Hz, 6H), 2.27 (s, 6H), 2.41 (q, $J =$ 6.0 Hz, 4H), 3.88 (s, 2H), 4.23 (q, $J =$ 7.3 Hz, 4H), 9.31 (brs, 2H) ppm; ^{13}C NMR (CDCl$_3$, δ, 75 MHz): 10.24 (q), 14.25 (q), 15.14 (q), 17.03 (t), 22.77 (t), 59.67 (t), 117.77 (s), 123.95 (s), 126.72 (s), 128.72 (s), 161.69 (s) ppm.

3,3′-Diethyl-4,4′-dimethyl-2,2′-dipyrryl ketone (**1**; $C_{15}H_{20}N_2O$)

Keto diester **5** [15b] (4.8 g, 0.124 mol) and 2 g, NaOH (0.05 mol, 4.1 equivs.) were dissolved in 80 cm^3 of 95% ethanol and 20 cm^3 H$_2$O. The mixture was heated at reflux for 3 h, and the solvent was evaporated (rotovap). The residue was taken up in 80 cm^3 sat. aqueous NaNO$_3$ solution, cooled to $-20°$C, and acidified to $pH \sim 6$ by adding a solution of 10% HCl (made up from conc. HCl and sat. aqueous NaNO$_3$ solution). The white diacid precipitate was collected by filtration and air dried to give a crude yield of 99%. The dried diacid (**4**, 100 mg, 0.3 mmol) was mixed with 3 g sodium acetate trihydrate and heated at 260°C for 1 h under vacuum (1 torr). After cooling to room temperature, the residue was washed with dichloromethane (2×50 cm^3), the combined organic phases were washed with 2×50 cm^3 sat. NaHCO$_3$ solution, and dried over anhydrous Na$_2$SO$_4$. After removing the CH$_2$Cl$_2$ (rotovap) the residue was recrystallized from CH$_2$Cl$_2$-hexane.

Yield: 51 mg (70%); m.p.: 180–182°C (Ref. [16]: m.p.: 180–180.5°C; IR (film): $\nu = 3254, 2967, 2934, 2853, 1576, 1560$ cm^{-1}; UV/Vis (ethanol): $\epsilon_{343}^{max} = 18000, \epsilon_{295}^{max} = 9900$; ^{1}H NMR (CDCl$_3$, δ,

Table 6. Crystallographic data for 2,2′-dipyrryl ketone **1**

Formula weight	488.7
Crystallized from	methanol-dichloromethane
Temperature (K)	298(2)
Crystal size (mm)	0.26×0.52×0.44
Formula	$C_{30}H_{40}N_4O_2$
Space group	P-1
Z	2
Cell dimensions	$a = 7.7330(8)$ Å
	$b = 12.1415(7)$ Å
	$c = 16.1395(17)$ Å
	$\alpha = 104.957(6)$
	$\beta = 97.106(9)$
	$\gamma = 102.834(10)$
	$V = 1400.8(2)$ Å
No/range of Refs. used for cell refinement	$26/5.09 < \theta < 12.41°$
Calc. density d_x (g/cm^3)	1.159
Data collection range	$3.5 < 2\theta < 50°$
Scan type / scan range	$\omega/1.1°$
No. Total data recorded	6027
No. Unique data	4859
Weighting scheme[a]	$a = 0.0603, b = 0.3677$
No. Obs. / no. parameters	4859 / 334
$R_1^b, wR_2^c (I > 2\sigma(I))$	$R_1 = 0.0511, wR_2 = 0.1270$
e.s.d. pf C–C bondlength	0.003
Highest peak in final ΔF map (e · Å^{-3})	0.166
Anisotropic non-H atoms	all
Isotropic non-H atoms	none
$\mu(MoK_\alpha)$ (mm^{-1})	0.073
Radiation (λ(Å))	0.71073
Transm. factors	0.9031−0.7919

[a] $w^{-1} = (\sigma^2(F_o^2) + (aP)^2 + bP)$ where $P = (F_o^2 + 2F_c^2)/3$; goodness of Fit (GOOF): $(\sum(w(F_o^2 - F_c^2)^2)/(M - N))^{0.5}$ where M is the number of reflections and N is the number of parameters refined; [b] $R_1 = (\sum | F_o | - | F_c |)/ \sum | F_o |$; [c] $wR_2 = (\sum[(w(F_o^2 - F_c^2)^2)/\sigma(w(F_o^2)^2)])^{0.5}$

300 MHz): 1.09 (t, $J = 7.3$ Hz, 6H), 2.08 (s, 6H), 2.63 (q, $J = 7.3$ Hz, 4H), 6.70 (d, $J = 4.4$ Hz, 2H), 8.58 (br s, 2H) ppm; ^{13}C NMR (CDCl$_3$, δ, 75 MHz): 9.73 (q), 15.04 (q), 17.95 (t), 120.26 (d), 120.36 (s), 128.17 (s), 131.73 (s), 174.44 (s) ppm.

X-Ray structure and solution

Crystals of 2,2′-dipyrryl ketone **1** were grown by slow diffusion of MeOH into a solution of CH$_2$Cl$_2$. Suitable crystals were coated with epoxy cement, mounted on a glass fiber, and placed on a Siemens

Table 7. Atomic coordinates ($\times 10^4$) and equivalent isotropic displacement parameters ($\mathring{A}^2 \times 10^3$) for **1**

	x	y	z	U(eq)[a]
O(1A)	10608(2)	9660(1)	2281(1)	48(1)
N(1A)	13093(2)	9087(2)	1194(1)	40(1)
N(2A)	7065(2)	8144(2)	1898(1)	40(1)
C(1A)	10148(3)	8740(2)	1642(1)	35(1)
C(2A)	11253(3)	8578(2)	985(1)	35(1)
C(3A)	10794(3)	8100(2)	73(1)	36(1)
C(4A)	12412(3)	8327(2)	−248(1)	43(1)
C(5A)	13788(3)	8918(2)	463(2)	47(1)
C(6A)	8494(3)	7848(2)	1563(1)	34(1)
C(7A)	8065(3)	6607(2)	1265(1)	38(1)
C(8A)	6331(3)	6183(2)	1427(1)	45(1)
C(9A)	5761(3)	7154(2)	1805(2)	48(1)
C(31A)	8946(3)	7587(2)	−489(1)	45(1)
C(32A)	8104(4)	8516(3)	−691(2)	82(1)
C(41A)	12600(4)	8020(3)	−1194(2)	67(1)
C(71A)	9269(4)	5850(2)	942(2)	52(1)
C(72A)	10484(5)	5674(3)	1679(2)	91(1)
C(81A)	5297(4)	4908(2)	1226(2)	68(1)
O(1B)	4082(2)	9763(1)	7275(1)	45(1)
N(1B)	6373(2)	8266(2)	6984(1)	45(1)
N(2B)	628(2)	9112(2)	6197(1)	44(1)
C(1B)	3614(3)	8855(2)	6629(1)	35(1)
C(2B)	4600(3)	7962(2)	6565(1)	37(1)
C(3B)	4050(3)	6720(2)	6250(1)	40(1)
C(4B)	5544(3)	6308(2)	6487(2)	47(1)
C(5B)	6943(3)	7283(2)	6924(2)	53(1)
C(6B)	2050(3)	8682(2)	5964(1)	36(1)
C(7B)	1639(3)	8159(2)	5056(1)	39(1)
C(8B)	−99(3)	8260(2)	4766(1)	46(1)
C(9B)	−668(3)	8840(2)	5483(2)	52(1)
C(31B)	2187(3)	5922(2)	5837(2)	48(1)
C(32B)	1079(5)	5701(4)	6498(2)	103(1)
C(41B)	5610(4)	5038(2)	6312(2)	70(1)
C(71B)	2833(4)	7690(2)	4468(1)	53(1)
C(72B)	3601(5)	8527(3)	3963(2)	83(1)
C(81B)	−1159(4)	7827(3)	3841(2)	70(1)

[a] U(eq) is defined as one third of the trace of the orthogonalized U_{ij} tensor, $U_{eq} = 1/3$ trace (U)

P4 diffractometer at room temperature. Unit cell parameters were determined by least squares analysis of 26 reflections with $5.09 < \theta < 12.41°$ using graphite monochromatized MoK_α radiation (0.71073 Å). 6027 reflections were collected between $3.5 < 2\theta < 50°$ yielding 4859 unique reflections ($R_{int} = 0.0247$). The data were corrected for *Lorentz* and polarization effects. Crystal data are given in Table 6. Scattering factors and corrections for anomolous dispersion were taken from a standard source [25]. Calculations were performed using a Siemens SHELXTL PLUS, version 5.03, system of programs refining on F^2. The structure was solved by direct methods in the space group P-1. The unit cell contains two crystallographically unique molecules that lie in an ordered array with no unusual contacts.

All non-hydrogen atoms (Fig. 3B, Table 7) were refined with anisotropic thermal parameters. The data were corrected using an empirical model derived from Ψ scans. Hydrogen atom positions were calculated using a riding model with a C-H distance fixed at 0.96 Å and a thermal parameter of 1.2 times that of the host carbon atom. The largest peak in the final difference map corresponded to 0.150 e$^-$/Å^3 and was located 1.2 Å from the C81 a carbon. Tables of bond lengths and angles, anisotropic displacement parameters, and isotropic displacement parameters have been deposited at the Cambridge Structural Data file (CCDC No. 43504).

Acknowledgements

References

[1] (a) Berk PD, Noyer C (1994) Seminars Liver Dis **14**: 323; (b) Chowdury JR, Wolkoff AW, Chowdury NR, Arias IM (1979) Hereditary Jaundice and Disorders of Bilirubin Metabolism. In: The Metabolic and Molecular Basis of Inherited Disease

[2] McDonagh AF (1979) Bile Pigments: Bilatrienes and 5,15-Biladienes. In: Dolphin D (ed) The Porphyrins. Academic Press, New York, Vol. 6, pp 293–491

[3] (a) Galliani G, Monti D, Speranza G, Manitto P, (1984) Tetrahedron Lett **25**: 6037; (b) Ostrow JD (1972) Seminars Hematol **9**: 113

[4] Falk H (1989) The Chemistry of Linear Oligopyrroles and Bile Pigments. Springer, Wien

[5] Bonnett R, Hursthouse MB, Neidle S (1972) J Chem Soc Perkin Trans 2, 1335

[6] (a) Bonnett R, Davies JE, Hursthouse MB, Sheldrick GM (1978) Proc R Soc London, Ser B **202**: 249; (b) LeBas G, Allegret A, Mauguen Y, DeRango C, Bailly M (1980) Acta Crystallogr, Sect B **B36**: 3007; (c) Becker W, Sheldrick WS (1978) Acta Crystallogr, Sect B **B34**: 1298

[7] (a) Cullen DL, Black PS, Meyer EF Jr, Lightner DA, Quistad GB, Pak CS (1977) Tetrahedron **33**: 477; (b) Cullen DL, Pèpe G, Meyer EF Jr, Falk H, Grubmayr K (1979) J Chem Soc Perkin 2, 999 (c) Hori A, Mangani S, Pèpe G, Meyer EF Jr, Cullen DL, Falk H, Grubmayr K (1981) J Chem Soc Perkin Trans 2, 1528

[8] (a) Favini G, Pitea D, Manitto P (1979) Nouv J Chem **3**: 299; (b) Falk H, Müller N (1983) Tetrahedron **39**: 1875; (c) Falk H (1986) Molecular Structure of Bile Pigments. In: Ostrow JD (ed) Bile Pigments and Jaundice. Dekker, New York, p 7; (d) Falk H, Höllbacher G, Hofer O, Müller N (1981) Monatsh Chem **112**: 391; Falk H, Müller N (1981) Monatsh Chem **112**: 1325

[9] Norsten TB, McDonald R, Branda NR (1999) J Chem Soc Chem Comm 719

[10] More M, Odou G, Lefebvre J (1987) Acta Crystallog **18**: 158

[11] Fischer H, Walach B (1926) Liebigs Ann Chem **450**: 109

[12] Shrout DP, Lightner DA (1990) Synthesis 1062

[13] Cheng LJ, Ma JS (1994) Synth Comm **24**: 2771
[14] Thyrann T, Lightner DA (1996) Tetrahedron Lett **37**: 315
[15] (a) Thyrann T, Lightner DA (1996) J Heterocyclic Chem **33**: 221; (b) Paine JB III, Dolphin DA (1976) Can J Chem **54**: 411
[16] Ogersby JM, MacDonald SF (1962) Can J Chem **40**: 1585
[17] Crusats J, Delgado A, Farrera JA, Rubires F, Ribó JM (1998) Monatsh Chem **129**: 741
[18] (a) Trull FR, Ma JS, Landen GL, Lightner DA (1983) Israel J Chem **23(2)**: 211; (b) Nogales DF, Ma JS, Lightner DA (1993) Tetrahedron **49**: 2361; (c) Boiadjiev SE, Anstine DT, Lightner DA (1995) J Am Chem Soc **117**: 8727; (d) Kar AK, Lightner DA (1998) Tetrahedron **54**: 5151
[19] Kuhn LP, Kleinspehn GG (1963) J Org Chem **28**: 721
[20] Jackman LM, Sternhell S (1969) Applications of Nuclear Magnetic Resonance Spectroscopy in Organic Chemistry. Pergamon Press, Oxford, UK, p 88–92
[21] Kikuchi H, Tsukitani Y, Yamada Y, Iguchi K, Drexler SA, Clardy J (1982) Tetrahedron Lett **23**: 1063
[22] Ma J, Chen Q, Cheng L, Wang C, Shen J (1995) Spectrosc Lett **28**: 223
[23] Rattini GA, Sleiter G (1975) Liebigs Ann Chem 1677
[24] Fischer H, Halbig P (1926) Liebigs Ann Chem **448**: 123, 193
[25] Ibers JA, Hamilton WC (1974) International Tables for X-ray Crystallography. Kynoch Press: Birmingham, England, Vol 4